

Barycentric interpolation and mappings on smooth convex domains

Michael S. Floater

Centre of Mathematics for Applications,
Department of Informatics, University of Oslo
PO Box 1053, Blindern
0316 Oslo, Norway
michaelf@ifi.uio.no

Jiří Kosinka

Centre of Mathematics for Applications,
Department of Informatics, University of Oslo
PO Box 1053, Blindern, 0316 Oslo, Norway
Department of Mathematics, Faculty of Applied
Sciences, University of West Bohemia
Univerzitní 8, 301 00 Plzeň, Czech Republic
jiri.kosinka@gmail.com

ABSTRACT

In a recent paper, Warren, Schaefer, Hirani, and Desbrun proposed a simple method of interpolating a function defined on the boundary of a smooth convex domain, using an integral kernel with properties similar to those of barycentric coordinates on simplexes. When applied to vector-valued data, the interpolation can map one convex region into another, with various potential applications in computer graphics, such as curve and image deformation. In this paper we establish some basic mathematical properties of barycentric kernels in general, including the interpolation property and a formula for the Jacobian of the mappings they generate. We then use this formula to prove the injectivity of the mapping of Warren et al.

Categories and Subject Descriptors

G.1.1 [Mathematics of Computing]: Numerical Analysis—*Interpolation*

General Terms

Theory, Design

Keywords

Interpolation, barycentric coordinates, barycentric mapping, injectivity.

1. INTRODUCTION

Generalizations of barycentric coordinates to arbitrary polygons and polyhedra have become a useful mathematical tool in various areas of computer graphics, such as shading, plane and space deformation, and animation. Mean value coordinates have emerged as a popular choice, due to their generality and surprising robustness over complex geometric shapes [5, 10, 18, 3, 7, 4, 8, 12, 15, 16]. For the specific case

of convex polygons and polyhedra, however, the coordinates of Wachspress and their generalizations due to Warren et al. [20, 22, 24, 13, 23] can be used instead, and the fact that they can be expressed in the form of rational functions can be viewed as an advantage; planar mean value coordinates involve square roots. We also now know [8] that barycentric mappings between convex polygons are always injective when based on Wachspress coordinates; in contrast, mean value coordinates can lead to fold-over, albeit in rather extreme cases. Related studies of barycentric coordinates and applications can be found in [6, 11, 15, 17, 21, 19, 25].

The main purpose of this paper is to investigate properties of the integral-based coordinates proposed by Warren, Schaefer, Hirani, and Desbrun [24] for convex sets with smooth boundary. These coordinates are a continuous analog of Wachspress coordinates; there is now one coordinate function for every point on the boundary curve, and one can view the whole set of coordinate functions as a single bivariate function that can be used as an integral kernel for interpolating data on the boundary. Our main result is to show that mappings between convex sets based on this kernel are always injective. In addition, we establish some basic mathematical properties of barycentric kernels in general, including the interpolation property and a formula for the Jacobian of the mappings they generate.

Let Ω be a bounded, open, strictly convex region of \mathbb{R}^2 with boundary $\partial\Omega$. By strict convexity we mean that no three points on $\partial\Omega$ are collinear. Suppose that $\mathbf{p} : [a, b] \rightarrow \mathbb{R}^2$, with $\mathbf{p}(a) = \mathbf{p}(b)$, is a continuous parametric representation of $\partial\Omega$, which is injective in $[a, b)$. Given a continuous function $f : \partial\Omega \rightarrow \mathbb{R}$ we are interested in finding an interpolant $g : \Omega \rightarrow \mathbb{R}$, i.e., a function with the property that for any $t \in [a, b)$,

$$g(\mathbf{x}) \rightarrow f(\mathbf{p}(t)) \quad \text{as } \mathbf{x} \rightarrow \mathbf{p}(t), \quad \text{for } \mathbf{x} \in \Omega.$$

One possible way of constructing such an interpolant is by an integral of the form

$$g(\mathbf{x}) = \int_a^b \lambda(\mathbf{x}, t) f(\mathbf{p}(t)) dt. \quad (1)$$

Here, we assume that both f and the kernel λ are continuous in t . As we will see there are various choices of the

kernel λ that guarantee the interpolation property: that g interpolates f .

One example is the Poisson kernel in the case that Ω is the unit disc. With $a = -\pi$, $b = \pi$, and $\mathbf{p}(t) = (\cos t, \sin t)$, the Poisson kernel is

$$\lambda(\mathbf{x}, t) = \frac{1 - \|\mathbf{x}\|^2}{2\pi(1 - 2\mathbf{x} \cdot \mathbf{p}(t) + \|\mathbf{x}\|^2)}.$$

It is well known [1] that in this case g is the unique harmonic extension of f to Ω , i.e., g is the solution to

$$\begin{aligned} \Delta g &= 0 & \text{in } \Omega, \\ g &= f & \text{in } \partial\Omega. \end{aligned}$$

An interesting alternative construction of this harmonic interpolant in terms of averages of linear interpolants to f was given in [9]. See also Section 3 of [2].

Recently, two kernels have been found that yield interpolation for any convex domain, with smooth enough boundary. Warren, Schaefer, Hirani, and Desbrun [24] proposed the kernel

$$\lambda(\mathbf{x}, t) = w(\mathbf{x}, t) / \int_a^b w(\mathbf{x}, s) ds, \quad (2)$$

where

$$w(\mathbf{x}, t) = \frac{\mathbf{p}'(t) \times \mathbf{p}''(t)}{((\mathbf{p}(t) - \mathbf{x}) \times \mathbf{p}'(t))^2}, \quad (3)$$

for domains for which $\mathbf{p} \in C^2[a, b]$, with \times denoting the cross product of vectors in \mathbb{R}^2 , i.e., $\mathbf{p} \times \mathbf{q} := p^1 q^2 - p^2 q^1$, where $\mathbf{p} = (p^1, p^2)$ and $\mathbf{q} = (q^1, q^2)$. Later, following the integral construction of mean value coordinates [5], a ‘mean value’ kernel was found [12, 4], namely (2) with w replaced by

$$w(\mathbf{x}, t) = \frac{(\mathbf{p}(t) - \mathbf{x}) \times \mathbf{p}'(t)}{\|\mathbf{p}(t) - \mathbf{x}\|^3},$$

which is defined for $\mathbf{p} \in C^1[a, b]$.

2. INTERPOLATION

We will say that the kernel λ in (1) is *barycentric* if for all $\mathbf{x} \in \Omega$,

$$\lambda(\mathbf{x}, t) \geq 0, \quad t \in [a, b], \quad (4)$$

$$\int_a^b \lambda(\mathbf{x}, t) dt = 1, \quad (5)$$

$$\int_a^b \lambda(\mathbf{x}, t) \mathbf{p}(t) dt = \mathbf{x}. \quad (6)$$

In this section we show that if λ is any barycentric kernel and f in (1) is continuous then g interpolates f . A crucial point that makes this work is the strict convexity of Ω .

We start by deriving a property of the coordinates that makes precise the intuitive idea that if λ is barycentric then $\lambda(\mathbf{x}, \cdot)$ converges to a delta function as \mathbf{x} converges to a boundary point. To show this we will use the *linear precision* property of such λ , namely that if L is some linear polynomial, $L(\mathbf{x}) = a_0 + a_1 x + a_2 y$, where $\mathbf{x} = (x, y)$, and $f = L|_{\partial\Omega}$ then $g = L|_{\Omega}$. This follows from the two equations (5) and (6).

LEMMA 1. *For any s_1, s, s_2 , with $a \leq s_1 < s < s_2 < b$, let $J = [a, b] \setminus [s_1, s_2]$. If λ is barycentric then, for $\mathbf{x} \in \Omega$,*

$$\int_J \lambda(\mathbf{x}, t) dt \rightarrow 0 \quad \text{as } \mathbf{x} \rightarrow \mathbf{p}(s).$$

PROOF. Let L be any infinite line passing through $\mathbf{p}(s)$ that lies to one side of Ω . Such a line must exist because Ω is convex. Then, for any $\mathbf{x} \in \Omega$ let $h(\mathbf{x})$ denote the perpendicular height of \mathbf{x} from L . Algebraically we can express h as the scalar product

$$h(\mathbf{x}) = \mathbf{n} \cdot (\mathbf{x} - \mathbf{p}(s)),$$

where \mathbf{n} is the unit vector perpendicular to L that points into Ω . Since h is a linear function, the linear precision property of λ implies that

$$h(\mathbf{x}) = \int_a^b \lambda(\mathbf{x}, t) h(\mathbf{p}(t)) dt.$$

Due to the non-negativity of $\lambda(\mathbf{x}, t)$ it follows that

$$h(\mathbf{x}) \geq \int_J \lambda(\mathbf{x}, t) h(\mathbf{p}(t)) dt.$$

Moreover, due to the convexity of Ω , we have, for $t \in J$,

$$h(\mathbf{p}(t)) \geq \min\{h(\mathbf{p}(s_1)), h(\mathbf{p}(s_2))\},$$

which is strictly positive due to the strictness of the convexity of Ω . Thus we have the upper bound,

$$\int_J \lambda(\mathbf{x}, t) dt \leq \frac{h(\mathbf{x})}{\min\{h(\mathbf{p}(s_1)), h(\mathbf{p}(s_2))\}},$$

and since $h(\mathbf{x}) \rightarrow 0$ as $\mathbf{x} \rightarrow \mathbf{p}(s)$, the lemma clearly follows. \square

Due to the lemma, we can now prove the interpolation property, using a similar approach to that of Theorem 4 of [4].

THEOREM 1. *If λ is barycentric and f is continuous then g interpolates f .*

PROOF. Let $\mathbf{p}(s)$ be any boundary point and let $\epsilon > 0$. Since $f \circ \mathbf{p}$ is continuous at $t = s$, we can choose $\gamma > 0$ small enough that $|f(\mathbf{p}(t)) - f(\mathbf{p}(s))| < \epsilon/2$ for $t \in I$, where $I = [s - \gamma, s + \gamma]$. Next, observe that for $\mathbf{x} \in \Omega$,

$$g(\mathbf{x}) - f(\mathbf{p}(s)) = \int_a^b \lambda(\mathbf{x}, t) (f(\mathbf{p}(t)) - f(\mathbf{p}(s))) dt.$$

We can split this integral into two parts, $\int_a^b = \int_I + \int_J$, where $J = [a, b] \setminus I$. Then, with $M := \sup_{\mathbf{y} \in \partial\Omega} |f(\mathbf{y})|$,

$$\begin{aligned} |g(\mathbf{x}) - f(\mathbf{p}(s))| &\leq \sup_{t \in I} |f(\mathbf{p}(t)) - f(\mathbf{p}(s))| \int_I \lambda(\mathbf{x}, t) dt \\ &\quad + 2M \int_J \lambda(\mathbf{x}, t) dt, \end{aligned}$$

and since $\int_I \lambda(\mathbf{x}, t) dt \leq 1$,

$$|g(\mathbf{x}) - f(\mathbf{p}(s))| < \frac{\epsilon}{2} + 2M \int_J \lambda(\mathbf{x}, t) dt.$$

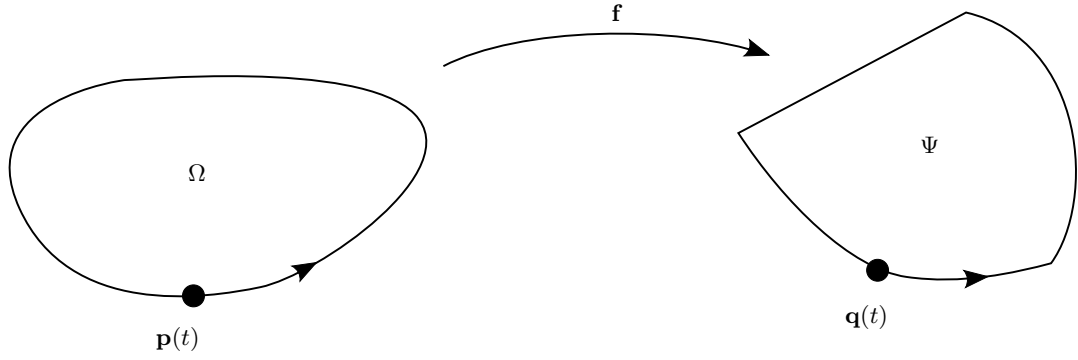


Figure 1: Barycentric mappings between convex domains.

By Lemma 1, there is some $\delta > 0$ such that if $\|\mathbf{x} - \mathbf{p}(s)\| \leq \delta$ then

$$\int_J \lambda(\mathbf{x}, t) dt < \frac{\epsilon}{4M},$$

in which case $|g(\mathbf{x}) - f(\mathbf{p}(s))| < \epsilon$. \square

3. BARYCENTRIC MAPPINGS

Let $\Psi \subset \mathbb{R}^2$ be a second convex domain, whose boundary $\partial\Psi$ is represented parametrically as $\mathbf{q} : [a, b] \rightarrow \mathbb{R}^2$, which is continuous and injective in $[a, b)$, with $\mathbf{q}(a) = \mathbf{q}(b)$. We can associate with any barycentric kernel λ a mapping $\mathbf{f} : \Omega \rightarrow \mathbb{R}^2$ by

$$\mathbf{f}(\mathbf{x}) = \int_a^b \lambda(\mathbf{x}, t) \mathbf{q}(t) dt, \quad \mathbf{x} \in \Omega. \quad (7)$$

By the interpolation property, if Ω is strictly convex we know that $\mathbf{f}(\mathbf{x}) \rightarrow \mathbf{q}(t)$ as $\mathbf{x} \rightarrow \mathbf{p}(t)$ for $\mathbf{x} \in \Omega$ and so we can continuously extend \mathbf{f} to $\partial\Omega$ by defining $\mathbf{f}(\mathbf{p}(t)) = \mathbf{q}(t)$. An important question though is whether \mathbf{f} is a one-to-one mapping from $\bar{\Omega}$ to $\bar{\Psi}$. Certainly, by the convexity of Ψ , the point $\mathbf{f}(\mathbf{x})$, being a weighted positive average of the boundary points $\mathbf{q}(t)$, must belong to Ψ , so \mathbf{f} maps $\bar{\Omega}$ to $\bar{\Psi}$. The remaining question is whether \mathbf{f} is injective. Assuming \mathbf{p} and \mathbf{q} are anticlockwise parameterizations, as in Fig. 1, the injectivity of \mathbf{f} reduces to the question of whether its Jacobian is positive in Ω . To help in answering this we derive a useful formula for the Jacobian, analogous to the one in [8]. Let $\mathbf{f}(\mathbf{x}) = (f(\mathbf{x}), g(\mathbf{x}))$, and $\partial_r h(\mathbf{x}) := \partial h / \partial x^r$, $r = 1, 2$. Then the Jacobian of \mathbf{f} is the determinant

$$J(\mathbf{f}) = \begin{vmatrix} \partial_1 f & \partial_1 g \\ \partial_2 f & \partial_2 g \end{vmatrix}.$$

For differentiable functions $h_1(\mathbf{x}), h_2(\mathbf{x}), h_3(\mathbf{x})$, let

$$\mathcal{D}(h_1, h_2, h_3) = \begin{vmatrix} h_1 & h_2 & h_3 \\ \partial_1 h_1 & \partial_1 h_2 & \partial_1 h_3 \\ \partial_2 h_1 & \partial_2 h_2 & \partial_2 h_3 \end{vmatrix}.$$

Moreover, we define $A(\mathbf{a}, \mathbf{b}, \mathbf{c})$ as the signed area of the triangle $[\mathbf{a}, \mathbf{b}, \mathbf{c}]$,

$$A(\mathbf{a}, \mathbf{b}, \mathbf{c}) = \frac{1}{2} \begin{vmatrix} 1 & 1 & 1 \\ a^1 & b^1 & c^1 \\ a^2 & b^2 & c^2 \end{vmatrix},$$

where $\mathbf{a} = (a^1, a^2)$, $\mathbf{b} = (b^1, b^2)$, $\mathbf{c} = (c^1, c^2)$.

LEMMA 2. If λ is a barycentric kernel, differentiable with respect to the second variable, then

$$J(\mathbf{f})(\mathbf{x}) = 2 \iint \int_{a \leq s < t < u \leq b} \mathcal{D}(\lambda(\mathbf{x}, s), \lambda(\mathbf{x}, t), \lambda(\mathbf{x}, u)) \times A(\mathbf{q}(s), \mathbf{q}(t), \mathbf{q}(u)) ds dt du.$$

PROOF. Differentiating (5) and (7) gives the matrix equation

$$\begin{pmatrix} 1 & f(\mathbf{x}) & g(\mathbf{x}) \\ 0 & \partial_1 f(\mathbf{x}) & \partial_1 g(\mathbf{x}) \\ 0 & \partial_2 f(\mathbf{x}) & \partial_2 g(\mathbf{x}) \end{pmatrix} = \begin{pmatrix} \int \lambda(\mathbf{x}, t) dt & \int \lambda(\mathbf{x}, t) q_1(t) dt & \int \lambda(\mathbf{x}, t) q_2(t) dt \\ \int \partial_1 \lambda(\mathbf{x}, t) dt & \int \partial_1 \lambda(\mathbf{x}, t) q_1(t) dt & \int \partial_1 \lambda(\mathbf{x}, t) q_2(t) dt \\ \int \partial_2 \lambda(\mathbf{x}, t) dt & \int \partial_2 \lambda(\mathbf{x}, t) q_1(t) dt & \int \partial_2 \lambda(\mathbf{x}, t) q_2(t) dt \end{pmatrix},$$

with $\mathbf{q}(t) = (q_1(t), q_2(t))$, and all integrals over $t \in [a, b]$. Therefore, $J(\mathbf{f})(\mathbf{x})$ is the determinant of the 3×3 matrix on the right hand side. We now use the integral version of the Cauchy-Binet theorem (c.f. [14], Formula (2.5)). For functions A_1, \dots, A_n and B_1, \dots, B_n , the theorem states that

$$\left| \left(\int_a^b A_i(t) B_j(t) dt \right)_{ij} \right| = \int_{a \leq t_1 \leq t_2 \leq \dots \leq t_n \leq b} |(A_j(t_i))_{ij}| |(B_j(t_i))_{ij}| dt_1 dt_2 \dots dt_n.$$

Putting $n = 3$ and letting $A_1(t) = \lambda(\mathbf{x}, t)$, $A_2(t) = \partial_1 \lambda(\mathbf{x}, t)$, $A_3(t) = \partial_2 \lambda(\mathbf{x}, t)$, and $B_1(t) = 1$, $B_2(t) = q_1(t)$, and $B_3(t) = q_2(t)$ in this formula gives the result. \square

Since all areas $A(\mathbf{q}(s), \mathbf{q}(t), \mathbf{q}(u))$ in Lemma 2 are positive this gives a sufficient condition for injectivity.

THEOREM 2. If

$$\mathcal{D}(\lambda(\mathbf{x}, s), \lambda(\mathbf{x}, t), \lambda(\mathbf{x}, u)) > 0$$

for all $\mathbf{x} \in \Omega$ and all $a \leq s < t < u \leq b$ then \mathbf{f} is injective.

4. THE MAPPING OF WARREN ET AL.

Consider now the barycentric kernel (2-3). The barycentric property (6) was established for this kernel in Section 3.2 of [24] as the special, planar case of a remarkable general

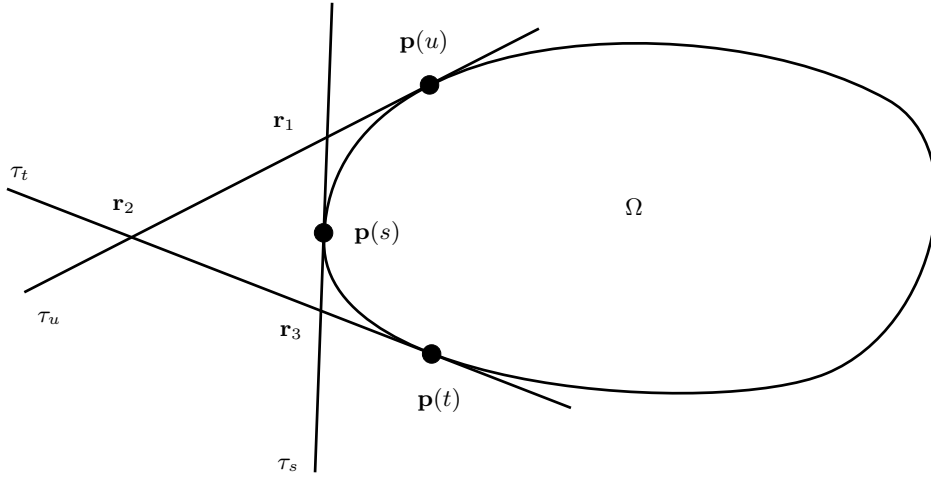


Figure 2: A triangle formed by three tangents of \mathbf{p} .

formula in arbitrary dimension involving Gauss curvature, which was proved using Stoke's theorem and an implicit representation of $\partial\Omega$. For the planar case, we have found a simpler proof of (6), which is as follows. We first note that due to the form of λ in (2), equation (6) is equivalent to

$$\int_a^b w(\mathbf{x}, t)(\mathbf{p}(t) - \mathbf{x}) dt = 0. \quad (8)$$

To show this we express the vector $\mathbf{p}(t) - \mathbf{x}$ as a linear combination of the two vectors $\mathbf{p}'(t)$ and $\mathbf{p}''(t)$:

$$\mathbf{p}(t) - \mathbf{x} = k(t)\mathbf{p}'(t) + l(t)\mathbf{p}''(t).$$

Taking the cross product of this equation first with $\mathbf{p}''(t)$, then with $\mathbf{p}'(t)$ gives the solutions

$$k(t) = \frac{(\mathbf{p}(t) - \mathbf{x}) \times \mathbf{p}''(t)}{\mathbf{p}'(t) \times \mathbf{p}''(t)}, \quad l(t) = -\frac{(\mathbf{p}(t) - \mathbf{x}) \times \mathbf{p}'(t)}{\mathbf{p}'(t) \times \mathbf{p}''(t)}.$$

It follows that

$$w(\mathbf{x}, t)(\mathbf{p}(t) - \mathbf{x}) = m(t)\mathbf{p}'(t) - n(t)\mathbf{p}''(t),$$

where

$$m(t) = \frac{(\mathbf{p}(t) - \mathbf{x}) \times \mathbf{p}''(t)}{((\mathbf{p}(t) - \mathbf{x}) \times \mathbf{p}'(t))^2}, \quad n(t) = \frac{1}{(\mathbf{p}(t) - \mathbf{x}) \times \mathbf{p}'(t)}.$$

Then, using the fact that

$$((\mathbf{p} - \mathbf{x}) \times \mathbf{p}')' = (\mathbf{p} - \mathbf{x}) \times \mathbf{p}'',$$

we have $n'(t) = -m(t)$. Hence

$$w(\mathbf{x}, t)(\mathbf{p}(t) - \mathbf{x}) = -(n\mathbf{p}')'(t),$$

and integrating this equation with respect to t from a to b gives (8) because $n(a)\mathbf{p}'(a) = n(b)\mathbf{p}'(b)$.

With the knowledge that the kernel (2-3) is barycentric, we are now ready to establish the injectivity of the mappings it generates.

THEOREM 3. *Let Ω be a strictly convex domain with a C^2 boundary curve and let Ψ be any convex domain. Then $\mathbf{f} : \bar{\Omega} \rightarrow \bar{\Psi}$ given by (7) and (2-3) is injective.*

PROOF. By Theorem 2 and Lemma 2 of [8] it is sufficient to show that

$$\mathcal{D}(w(\mathbf{x}, s), w(\mathbf{x}, t), w(\mathbf{x}, u)) > 0$$

for all $a \leq s < t < u \leq b$ and for all $\mathbf{x} \in \Omega$, with w in (3). The main steps of the proof are now similar to those in the proof of Theorem 3 of [8]. One can see that

$$\begin{aligned} \mathcal{D}(w(\mathbf{x}, s), w(\mathbf{x}, t), w(\mathbf{x}, u)) &= w(\mathbf{x}, s)\nabla w(\mathbf{x}, t) \times \nabla w(\mathbf{x}, u) \\ &\quad + w(\mathbf{x}, t)\nabla w(\mathbf{x}, u) \times \nabla w(\mathbf{x}, s) \\ &\quad + w(\mathbf{x}, u)\nabla w(\mathbf{x}, s) \times \nabla w(\mathbf{x}, t), \end{aligned}$$

where $\nabla w := (\partial_1 w, \partial_2 w)$, and a simple calculation shows that

$$\nabla w(\mathbf{x}, t) = w(\mathbf{x}, t) \frac{-2\mathbf{p}'(t)^\perp}{(\mathbf{p}(t) - \mathbf{x}) \times \mathbf{p}'(t)},$$

where $\mathbf{p}^\perp = (-p^2, p^1)$. It follows that

$$\nabla w(\mathbf{x}, s) \times \nabla w(\mathbf{x}, t) = 4w(\mathbf{x}, s)w(\mathbf{x}, t)R(s, t),$$

where

$$R(s, t) = \frac{\mathbf{p}'(s) \times \mathbf{p}'(t)}{((\mathbf{p}(s) - \mathbf{x}) \times \mathbf{p}'(s))((\mathbf{p}(t) - \mathbf{x}) \times \mathbf{p}'(t))},$$

and consequently

$$\frac{\mathcal{D}(w(\mathbf{x}, s), w(\mathbf{x}, t), w(\mathbf{x}, u))}{w(\mathbf{x}, s)w(\mathbf{x}, t)w(\mathbf{x}, u)} = 4(R(t, u) + R(u, s) + R(s, t)).$$

So, in analogy to the proof of Theorem 3 in [8], the task is to show that the sum of the three terms $R(u, s)$, $R(s, t)$, and $R(t, u)$ is positive. By the convexity of Ω and the ordering $s < t < u$, at least two of these terms must be positive. Thus, without loss of generality, it is sufficient to show that the sum is positive in the case that $R(u, s) > 0$, $R(s, t) > 0$, and $R(t, u) < 0$, as illustrated in Fig. 2. Then, with τ_t denoting the tangent line at $\mathbf{p}(t)$, consider the three lines τ_s, τ_t, τ_u . They intersect in three points: \mathbf{r}_1 the intersection of τ_u and τ_s ; \mathbf{r}_2 the intersection of τ_u and τ_t ; and \mathbf{r}_3 the intersection of τ_s and τ_t . Then, it is easy to see that

$$R(t, u) = \frac{(\mathbf{r}_3 - \mathbf{r}_2) \times (\mathbf{r}_2 - \mathbf{r}_1)}{((\mathbf{p}(t) - \mathbf{x}) \times (\mathbf{r}_3 - \mathbf{r}_2))((\mathbf{p}(u) - \mathbf{x}) \times (\mathbf{r}_2 - \mathbf{r}_1))}$$

and thus

$$R(t, u) = -\frac{A(\mathbf{r}_1, \mathbf{r}_2, \mathbf{r}_3)}{2A(\mathbf{x}, \mathbf{r}_2, \mathbf{r}_3)A(\mathbf{x}, \mathbf{r}_1, \mathbf{r}_2)},$$

$$R(u, s) = \frac{A(\mathbf{r}_1, \mathbf{r}_2, \mathbf{r}_3)}{2A(\mathbf{x}, \mathbf{r}_1, \mathbf{r}_2)A(\mathbf{x}, \mathbf{r}_1, \mathbf{r}_3)},$$

$$R(s, t) = \frac{A(\mathbf{r}_1, \mathbf{r}_2, \mathbf{r}_3)}{2A(\mathbf{x}, \mathbf{r}_1, \mathbf{r}_3)A(\mathbf{x}, \mathbf{r}_2, \mathbf{r}_3)},$$

and hence

$$R(t, u) + R(u, s) + R(s, t) = \frac{A(\mathbf{r}_1, \mathbf{r}_2, \mathbf{r}_3)^2}{2A(\mathbf{x}, \mathbf{r}_1, \mathbf{r}_2)A(\mathbf{x}, \mathbf{r}_2, \mathbf{r}_3)A(\mathbf{x}, \mathbf{r}_1, \mathbf{r}_3)} > 0.$$

□

5. EXAMPLES

In this section we illustrate our results by several examples.

The interpolation property of the kernel (2–3) is demonstrated in Fig. 3 a). Fig. 3 b) depicts a mapping between strictly convex domains generated by it. The small circles denote points with the same parameter values. Several curves similar in shape to the domain boundary and their images are depicted too. Since the image curves do not mutually intersect, the figure confirms the injectivity of the mapping.

Now consider the situation depicted in Fig. 4, top left. The domain boundary is given by a C^2 cubic spline curve whose control polygon is shown as well. By moving the control points of the spline curve the domain is deformed accordingly. Several such deformations (taken from an animation) are shown in Fig. 4. Observe in the last frame (bottom right) that the deformation is no longer injective.

6. REFERENCES

- [1] S. Axler, P. Bourdon, and W. Ramey. *Harmonic Function Theory*. Springer-Verlag, 1992.
- [2] A. Belyaev. On transfinite barycentric coordinates. In *Eurographics symposium on geometry processing*, pages 89–99. Eurographics Association, 2006.
- [3] S. Bruvold, and M. S. Floater. Transfinite mean value interpolation in general dimension. *Journal of Computational and Applied Mathematics*, 233(7):1631–1639, February 2010.
- [4] C. Dyken and M. S. Floater. Transfinite mean value interpolation. *Comp. Aided Geom. Design*, 26(1):117–134, January 2009.
- [5] M. S. Floater. Mean value coordinates. *Comp. Aided Geom. Design*, 20(1):19–27, March 2003.
- [6] M. S. Floater, K. Hormann, and G. Kós. A general construction of barycentric coordinates over convex polygons. *Adv. in Comp. Math.*, 24(1–4):311–331, January 2006.
- [7] M. S. Floater, G. Kós, and M. Reimers. Mean value coordinates in 3D. *Comp. Aided Geom. Design*, 22(7):623–631, October 2005.
- [8] M. S. Floater and J. Kosinka. On the injectivity of Wachspress and mean value mappings between convex polygons. *Adv. in Comp. Math.*, 32(2):163–174, February 2010.
- [9] W. J. Gordon and J. A. Wixom. Pseudo-harmonic interpolation on convex domains. *SIAM J. Numer. Anal.*, 11(5):909–933, October 1974.
- [10] K. Hormann and M. S. Floater. Mean value coordinates for arbitrary planar polygons. *ACM Trans. on Graph.*, 25(4):1424–1441, October 2006.
- [11] P. Joshi, M. Meyer, T. DeRose, B. Green, and T. Sanocki. Harmonic coordinates for character articulation. *ACM Trans. on Graph.*, 26(3):71, July 2007.
- [12] T. Ju, S. Schaefer, and J. Warren. Mean value coordinates for closed triangular meshes. *ACM Trans. on Graph.*, 24:561–566, August 2005.
- [13] T. Ju, S. Schaefer, J. Warren, and M. Desburn. A geometric construction of coordinates for convex polyhedra using polar duals. In *Eurographics Symposium on Geometry Processing*, pages 181–186. Eurographics Association, 2005.
- [14] S. Karlin. *Total positivity*. Vol. I, Stanford University Press, Stanford, CA, 1968.
- [15] T. Langer, A. Belyaev, and H.-P. Seidel. Spherical barycentric coordinates. In *Eurographics symposium on geometry processing*, pages 81–88. Eurographics Association, 2006.
- [16] T. Langer, A. Belyaev, and H.-P. Seidel. Mean value coordinates for arbitrary spherical polygons and polyhedra in \mathbb{R}^3 . In *Modern Methods in Mathematics*, pages 193–202. Avignon, 2007.
- [17] T. Langer and H.-P. Seidel. Higher order barycentric coordinates. *Computer Graphics Forum (Proc. Eurographics)*, 27(2):459–466, April 2008.
- [18] Y. Lipman, J. Kopf, D. Cohen-Or, and D. Levin. GPU-assisted positive mean value coordinates for mesh deformation. In *Eurographics Symposium on Geometry Processing*, pages 117–123. Eurographics Association, 2007.
- [19] Y. Lipman, D. Levin, and D. Cohen-Or. Green Coordinates. *ACM Trans. on Graph.*, 27(3):1–10, August 2008.
- [20] M. Meyer, A. Barr, H. Lee, and M. Desbrun. Generalized barycentric coordinates on irregular polygons. *Journal of graphics tools*, 7(1):13–22, November 2002.
- [21] S. Schaefer, T. Ju, and J. Warren. A unified integral construction for coordinates over closed curves. *Comp. Aided Geom. Design*, 24(8–9):481–493, November 2007.
- [22] E. L. Wachspress. *A rational finite element basis*. Academic Press, New York, 1975.
- [23] J. Warren. Barycentric coordinates for convex polytopes. *Adv. in Comp. Math.*, 6(1):97–108, December 1996.
- [24] J. Warren, S. Schaefer, A. Hirani, and M. Desbrun. Barycentric coordinates for convex sets. *Adv. in Comp. Math.*, 27(3):319–338, October 2007.
- [25] O. Weber, M. Ben-Chen, and C. Gotsman. Complex barycentric coordinates with applications to planar shape deformation. *Computer Graphics Forum (Proc. Eurographics)*, 28(2):587–597, 2009.

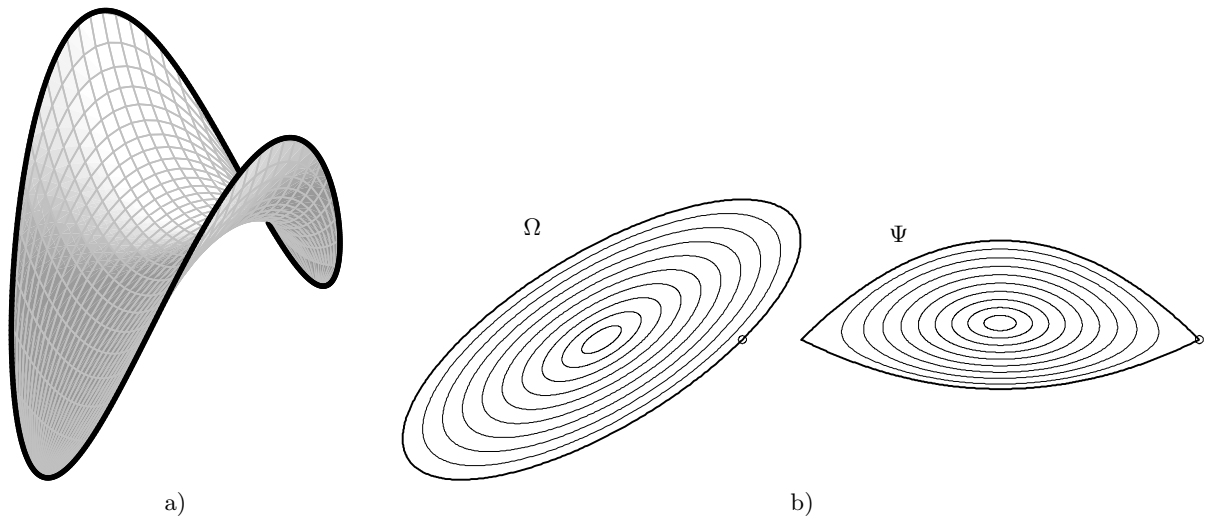


Figure 3: A barycentric interpolant and a barycentric mapping between convex domains.

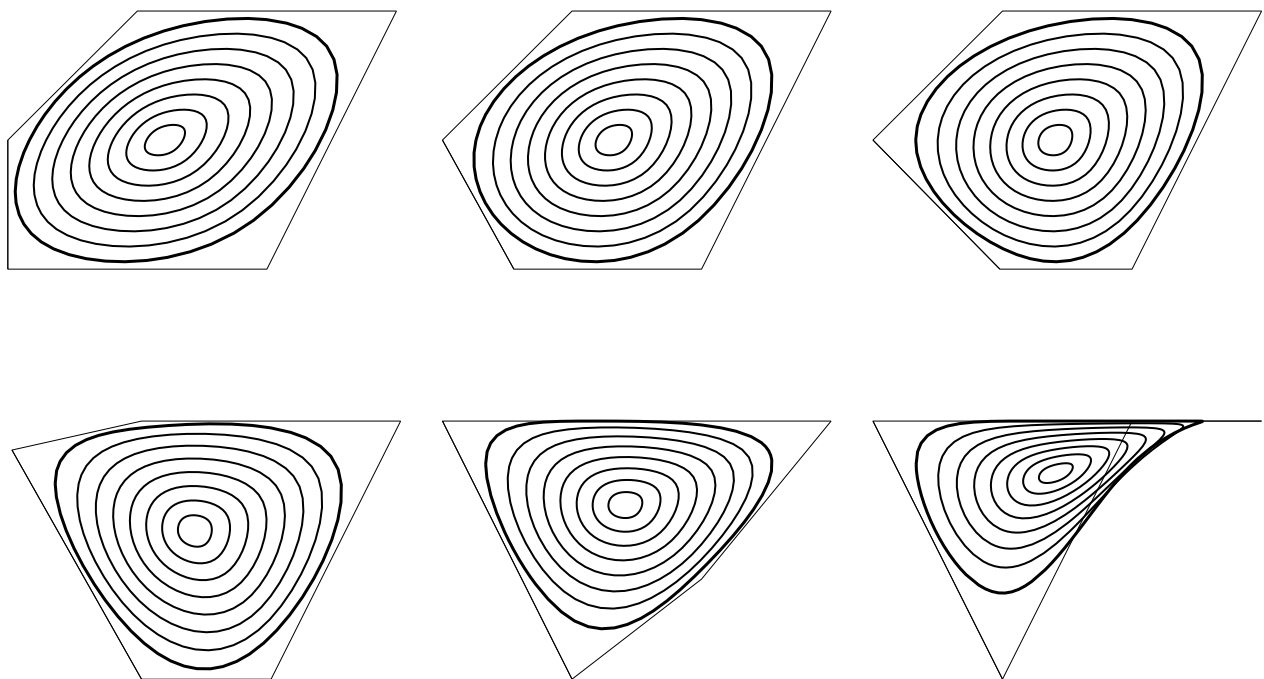


Figure 4: A sequence of figures corresponding to several frames of an animation. Top left shows the original shape, the others various deformations of the shape. Bottom right depicts a concave shape inducing a non-injective deformation.